Organic Electronics 13 (2012) 121–128

Contents lists available at SciVerse ScienceDirect

Organic Electronics

journal homepage: www.elsevier.com/locate/orgel

Role of geometry, substrate and atmosphere on performance of OFETs based on TTF derivatives

T. Marszalek [a,*], A. Nosal [b], R. Pfattner [c], J. Jung [a], S. Kotarba [a], M. Mas-Torrent [c], B. Krause [d,e], J. Veciana [c], M. Gazicki-Lipman [b], C. Crickert [f], G. Schmidt [g], C. Rovira [c], J. Ulanski [a]

[a] Department of Molecular Physics and European Centre for Bio- and Nanotechnology, Technical University of Lodz, 90-924 Lodz, Poland
[b] Institute of Mechanical Engineering, Technical University of Lodz, 90-924 Lodz, Poland
[c] Institut de Ciencia de Materials de Barcelona (ICMAB-CSIC) and (CIBER-BBN), Campus UAB, 08193 Bellaterra, Spain
[d] European Synchrotron Radiation Facility, ESRF BP 220 F-38043, Grenoble Cedex, France
[e] Karlsruher Institut für Technologie (KIT), Institut für Synchrotronstrahlung (ISS), 76344 Eggenstein-Leopoldshafen, Germany
[f] Universität Würzburg, Physikalisches Institut (EP3), Am Hubland, D-97074 Würzburg, Germany
[g] Universität Halle, Insitut für Physik, Von-Danckelmann-Platz 3, 06120 Halle, Germany

ARTICLE INFO

Article history:
Received 22 March 2011
Received in revised form 20 September 2011
Accepted 1 October 2011
Available online 20 October 2011

Keywords:
Tetrathiafulvalene derivatives
Organic field-effect transistors
Thin films
Organic transistor

ABSTRACT

We report a comparative study of OFET devices based on zone-cast layers of three tetrathiafulvalene (TTF) derivatives in three configurations of electrodes in order to determine the best performing geometry. The first testing experiments were performed using SiO_2/Si substrates. Then the optimum geometry was employed for the preparation of flexible OFETs using Parylene C as both substrate and dielectric layer yielding, in the best case, to devices with $\mu_{FET} = 0.1$ cm^2/V s. With the performed bending tests we determined the limit of curvature radius for which the performance of the OFETs is not deteriorated irreversibly. The investigated OFETs are sensitive to ambient atmosphere, showing reversible increase of the source to drain current upon exposition to air, what can be explained as doping of TTF derivative by oxygen or moisture.

1. Introduction

In the area of organic field effect transistors (OFETs) huge progress has been achieved and high mobility up to 20 cm^2/V s was reported for devices based on single crystals of rubrene [1]. Interesting p-type semiconductors applied as active material in OFETs are tetrathiafulvalene (TTF) derivatives, which show a remarkable device performance and facile processability [2]. Solution grown single crystals of this family of compounds have given rise to mobilities in the order of 1–10 cm^2/V s [3–5]. However, small size and poor mechanical properties of single crystals limit their practical applications in organic large area electronics (OLAE). Because of the strong correlation between the crystal structure and the device performance methods of controlled layer deposition are needed. One of such methods is the zone-casting technique [6], which allows to produce highly ordered layers of "p" and "n" type low molecular weight semiconductors [7–9] and discotic liquid crystals [10,11].

Interest in flexible dielectrics and supports suitable for OFETs has been rapidly growing in recent years [12]. Using the unique properties of the polymer Parylene C one can take advantage of the parylene technology to produce support, dielectric and encapsulating layers using the same insulator polymer [13].

In this paper we describe a strategy to optimize the process of fabrication of flexible OFETs based on highly ordered TTF-based active layers produced by zone-casting. First, the best electrodes configuration for the transistors was determined employing rigid silicon wafers as support. Then, using the optimized devices geometry, flexible OFETs were produced using three TTF derivatives as active

* Corresponding author.
E-mail address: tomasz.marszalek@p.lodz.pl (T. Marszalek).

1566-1199/$ - see front matter © 2011 Elsevier B.V. All rights reserved.
doi:10.1016/j.orgel.2011.10.001

material and Parylene C as both substrate and dielectric. We have investigated also the influence of ambient atmosphere on the performance of the latter OFETs.

2. Materials and methods

The molecular structures of TTF-4SC$_n$ (n = 12, 18, and 22), which were synthesized following the methodology reported by Wu et al. [14], are presented in Fig. 1. These small π-conjugated molecules show a strong tendency for quasi 1-dimensional π–π-stacking and close sulfur–sulfur interactions between adjacent molecules. Such structural characteristics favor the production of highly ordered polycrystalline layers on large areas using solution-based zone-casting techniques [15,7] and are responsible for the outstanding charge transport properties of TTF-derivatives. The zone-casting method consists in pouring the solution of the semiconductors molecule via flat nozzle onto a moving substrate. When the casting parameters – solution concentration and temperature, solution dosing rate, temperature of the substrate, substrate moving speed are optimized, it is possible to obtain large area (several square centimeters), highly oriented layer of organic semiconductors showing crystals – like structure [7,10].

Fig. 2 shows the chemical structure of Parylene C, which was used as flexible substrate and as gate dielectric in the fabricated OFETs.

2.1. Role of electrodes configuration. Fabrication and characterization of devices based on flexible substrate

It was found before, that the best results one can get with zone-cast semiconductors are for bottom gate, top contact configuration, because the contacts are not disturbing the organization of the deposited semiconductor layers, caused by geometrical effects or due to differences in surface energy of metal and dielectric. In order to determine the best architecture for high performing devices based on the zone-cast films, transistors in three configurations of source, drain electrodes were prepared on highly doped silicon wafers Si/SiO$_2$ with thermally grown silicon oxide and using the same organic semiconductor TTF-4SC$_{22}$:

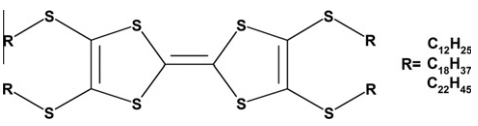

Fig. 1. Chemical structure of tetrakis(alkylthio)tetrathiafulvalenes – TTF-4SC$_n$, where: n = 12, 18, and 22.

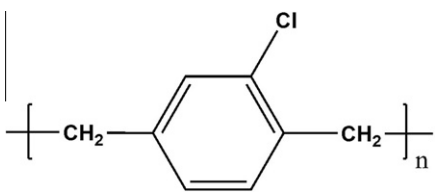

Fig. 2. Chemical structure of Parylene C.

In the first case a top contact–bottom gate (TC,BG) architecture with 150 nm of thermally grown SiO$_2$ as a dielectric was used (Fig. 3a), while for the second experiment we employed a bottom contact – bottom gate (BC,BG) geometry and a 50 nm thick SiO$_2$ dielectric (Fig. 3b). In the third case a (BC,BG) configuration (50 nm of SiO$_2$) was also used but here buried source-drain electrodes were fabricated by a photolithography process followed by a wet chemical etching using buffered HF (Fig. 3c). The source and drain electrodes were evaporated and consisted of about 120 nm of Au for the first configuration where the channel width/length ratio was 25 and 1 nm of Ti and 19 nm of Au for the other two cases where the channel width/length ratio was 1000. Highly oriented layers of TTF-4SC$_{22}$ were prepared by zone-casting using a solution (conc. = 1.5 mg/ml in chlorobenzene), on Si/SiO$_2$ substrates. To dissolve the TTF completely, the solution was heated up to 50 °C. The best ordered layers were obtained with the substrate velocity about 8 μm/s. The solution temperature was kept constant at 83 °C, while the substrate temperature was maintained at 78 °C.

After optimization of the source drain configuration the flexible OFETs were produced. First a 10 μm thick Parylene C film (used as substrate) was formed on top of freshly cleaned glass plate by chemical vapor deposition. Then a 120 nm thick Au gate electrode was evaporated and followed by the deposition of a second ca. 1 μm thick Parylene C layer (used as dielectric ε = 3.15). After the fabrication process, the flexible organic field-effect transistor, can be detached from the glass support.

The oriented layers of TTF-4SC$_n$ on Parylene C dielectric were prepared by the zone-casting technique with the casting parameters optimized for this substrate. The layers of TTF-4SC$_{12}$ and TTF-4SC$_{18}$ were prepared from toluene solution (conc. = 2 mg/ml) and the TTF-4SC$_{22}$ from chlorobenzene solution (conc. = 1.5 mg/ml). The substrate velocity was constant at 20 μm/s. The temperature of the supplied solutions was fixed at 80 °C, while the substrate temperature was kept constant at 76 °C.

The quality of the obtained semiconductor layers was examined by Polarized Optical Microscopy (POM) (Bipolar microscope, PZO), Atomic Force Microscopy (AFM) (SOLVER PRO scanning probe microscope, NT-MDT) and UV-Vis absorption spectroscopy (Varian Cary 5000 UV–Vis-NIR spectrometer).

OFETs based on TTF-4SC$_n$ as active material and Parylene C as dielectric were fabricated applying the top contact–bottom gate configuration. The source and drain Au electrodes (thickness ca. 120 nm) were evaporated on top of the TTF-4SC$_n$ layer, with the channel either parallel or perpendicular to the zone-casting direction. Anisotropy of electrical properties was analyzed calculating the charge carrier mobility μ_{FET}. The devices were produced and measured under ambient conditions (room temperature: $T \sim 26$ °C, relative humidity: RH ~ 28–36%). Using relation (1) the field-effect mobility was calculated in the saturation regime. More than 20 FETs were produced and tested, showing a remarkable reproducibility in their performance.

$$\mu_{SAT} = \frac{2L}{WC_i}\left(\frac{\partial\sqrt{I_{DS,SAT}}}{\partial V_{GS}}\right)^2 \quad (1)$$

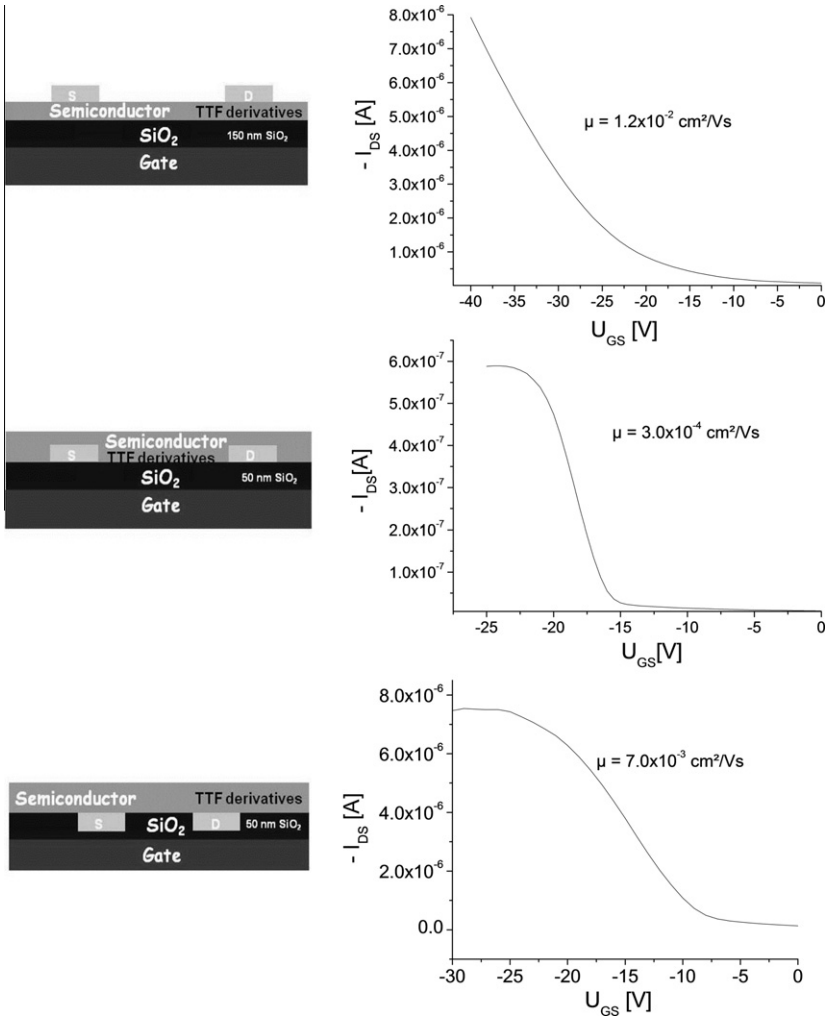

Fig. 3. Transfer characteristics of OFETs made of TTF-4SC$_{22}$ zone-cast on Si/SiO$_2$ substrates with different configuration of electrodes: (a) top contacts, bottom gate; (b) bottom contacts, bottom gate; (c) bottom contacts, bottom gate – buried electrodes.

where: L – channel length; W – channel width; V_{GS} – source-gate voltage; $I_{DS,SAT}$ – source–drain current; C_i – gate capacitance.

3. Results and discussion

3.1. OFETs with zone-cast TTF-4SC$_{22}$ layer on Si/SiO$_2$ substrates

The influence of the electrode architecture on the device performance of OFETs with zone-cast TTF-4SC$_{22}$ layers was explored by evaluating the charge carrier mobility μ_{FET}. The highest charge carrier mobilities were found for the OFETs on Si/SiO$_2$ and the (TC,BG) structure (Fig. 3a): $\mu_{FET} = 0.012$ cm^2/V s. Slightly lower mobility for the OFETs with bottom buried contacts (Fig. 3c, $\mu_{FET} = 0.007$ cm^2/V s) can result from differences in the substrate wettability and in the surface energy between Si/SiO$_2$ and gold electrodes that can induce structural modifications. For the OFETs with evaporated bottom contacts, the mobility was found to be lower (Fig. 3b, $\mu_{FET} = 0.0003$ cm^2/V s) which can be attributed to the corrugated surface of the substrate with evaporated electrodes disturbing ordering of the TTF-4SC$_{22}$ layer, as previously found for another TTF derivative [16]. In Fig. 4 one can see discontinuity of the zone-cast layer apparently caused by gold electrodes evaporated on top of the Si/SiO$_2$ substrate.

The effect of surface energy on the device performance was described by Miskiewicz et al. [17]. The morphology of the substrate surface was found to be very important. The best homogenous films prepared by zone-cast were obtained on very smooth Si/SiO$_2$ substrates (roughness less than 3 nm), in which needle-shaped crystallites (with a typical length of 150–200 μm, width of 5–15 μm) were observed.

The crystalline structure of the TTF-4SC$_{22}$ zone-cast film on smooth Si/SiO$_2$ substrate was studied by X-ray diffraction. The results of the reflectivity measurements are shown in Fig. 5. The X-ray diffraction spectrum is not as perfect as those obtained before for TTF-4SC$_{18}$ layer [8],

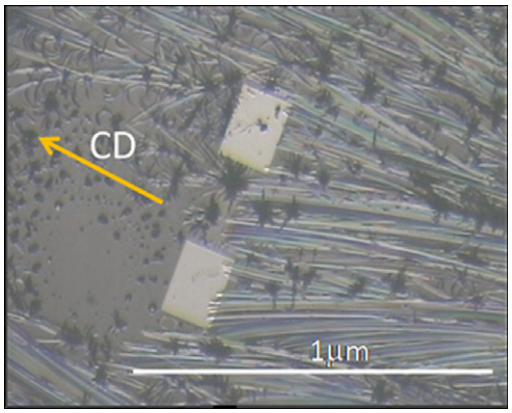

Fig. 4. Optical microscope image of a device based on TTF-4SC$_{22}$ layer with gold source and drain electrodes evaporated on Si/SiO$_2$ (BC,BG). Arrow CD – casting direction.

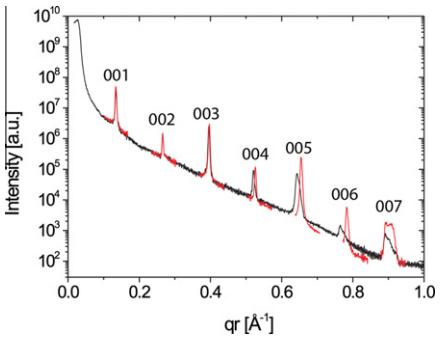

Fig. 5. Reflectivity measurement (black line) and measurements of the individual Bragg peaks (red line). (For interpretation of the references to color in this figure legend, the reader is referred to the web version of this article.)

due to damage of the sample caused by X-Ray beam, resulting in broadening and shift of the Bragg peaks. One should remember also, that for this family of TTF derivatives it is very difficult to get crystals perfect enough to determine their crystals structure. So far only for TTF-4SC$_n$ with $n < 9$ it was possible to determine the single crystals structure [23]. Nevertheless the realized experiments were highly reproducible, supporting the hypothesis of long-range homogeneity and high crystalline ordering of the zone-cast TTF-4SC$_{22}$ films. The spacing of monomolecular layers, $d = 47.5$ Å, was determined from the Bragg peak positions of the (001), (002), and (003) diffraction peaks. This distance points out that the TTF-4SC$_{22}$ molecules are arranged with their long axis aligned almost perpendicular to the surface. One can conclude thus that the molecular stacking direction which forms the conduction channel is parallel to the substrate, which is a crucial requirement for the preparation of high performing OFETs.

Fig. 6 shows the radial in-plane diffraction measurements performed under grazing incidence angle $\alpha i = 0.065°$. The measurements in casting direction (black line) and perpendicular to the casting direction (red line) differ significantly. Peak 1 observed perpendicular to the casting direction at $q = 0.12$ Å^{-1} belongs to the peak group

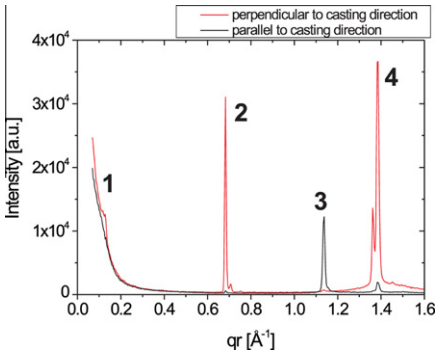

Fig. 6. Radial in-plane diffraction measurement parallel (black line) and perpendicular (red line) to the casting direction. (For interpretation of the references to color in this figure legend, the reader is referred to the web version of this article.)

observed in the reflectivity measurements. Its low intensity indicates again that nearly all molecules are standing upright on the surface. The peak 2 at $q = 0.682$ Å^{-1} observed perpendicular to the casting direction and 3 at $q = 1.137$ Å^{-1} (corresponding to $d = 5.5$ Å) indicates that the molecular stacking direction is along the casting direction. The peak 2 is a (100) peak corresponding to $d = 9.2$ Å, and peak 3 is a (010) peak corresponding to $d = 5.5$ Å.

On other hand in the reciprocal space maps shown in Fig. 7 it is observed that, both in the casting direction and perpendicular to it, a vertical row of peaks is visible, confirming the high crystalline order of the sample.

Analyzing the values of mobility one can conclude, that for OFETs with the zone-cast TTF-4SC$_n$ layers, the highest charge carrier mobility (μ_{FET}) and the highest source-drain current I_{DS} was observed for the top contact configuration due to the fact that the homogeneous, smooth substrate do not disturb the growing of the TTF-4SC$_n$ layer.

3.2. FETs with the zone-cast TTF-4SC$_n$ layers on Parylene C substrates

Fig. 8 shows the polarized optical microscopy images of three TTF-4SC$_n$ ($n = 12$, 18, and 22) derivatives zone-cast on Parylene C substrate. The zone-cast layers exhibit optical birefringence and one can see long crystalline needles growing along the casting direction.

Taking into account the results described in the previous section, the OFET devices based on the zone-cast TTF-4SC$_n$ layers and Parylene C dielectric were fabricated on the top contact–bottom gate configuration. The source and drain Au electrodes (ca. 120 nm thick) were evaporated on top of the TTF-4SC$_n$ layers, with channel orientated either parallel or perpendicular to the zone-casting direction. Anisotropy of the electrical properties were characterized analyzing the charge carrier mobility. The OFETs for all TTF derivatives with Parylene C as dielectric exhibit typical p-type behavior, as demonstrated by the output characteristics shown in Fig. 9. All OFETs prepared with zone-cast layers of ca. 8 cm^2 area exhibit similar performances with well reproducible charge carrier mobility.

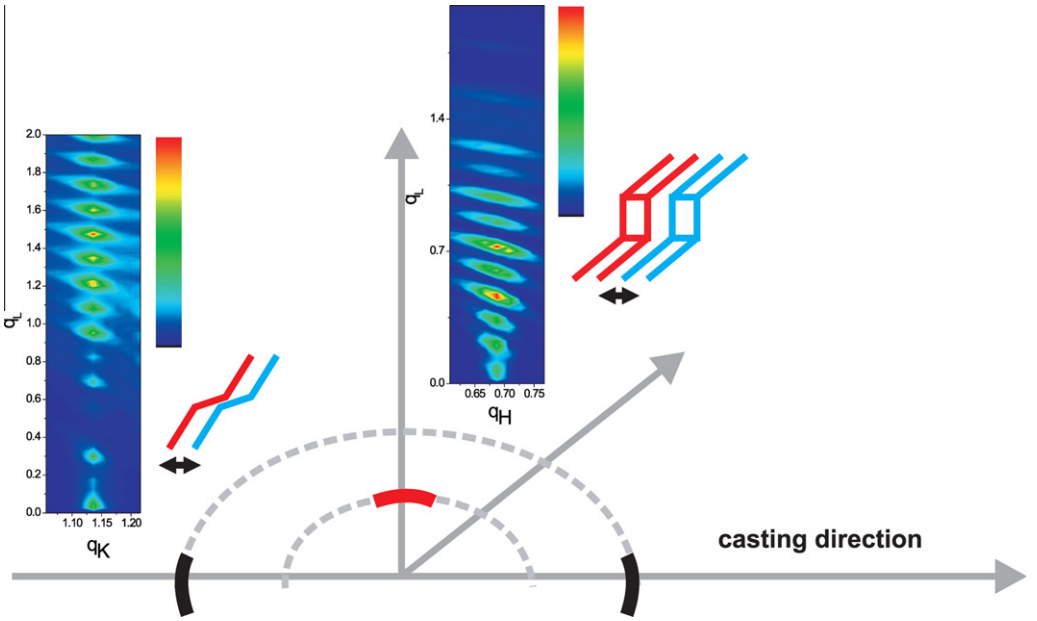

Fig. 7. Reciprocal space maps covering the radial direction in-plane (sensitive to the in-plane molecular stacking) and the out-of-plane direction (sensitive to the out-of-plane molecular stacking).

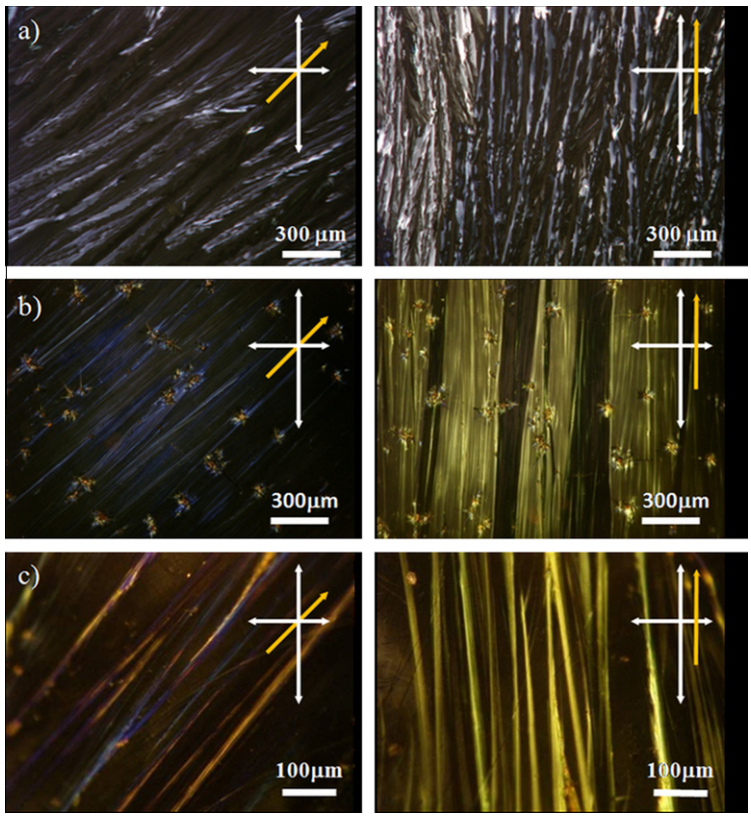

Fig. 8. Polarised Optical Microscope images (transmission mode) of the zone-cast TTF-4SC$_n$ layers on the Parylene C substrate, where (a) n = 12; (b) n = 18; (c) n = 22. Yellow arrows indicate the casting direction, white arrows show orientations of polarization planes of polarizer and analyzer. (For interpretation of the references to color in this figure legend, the reader is referred to the web version of this article.)

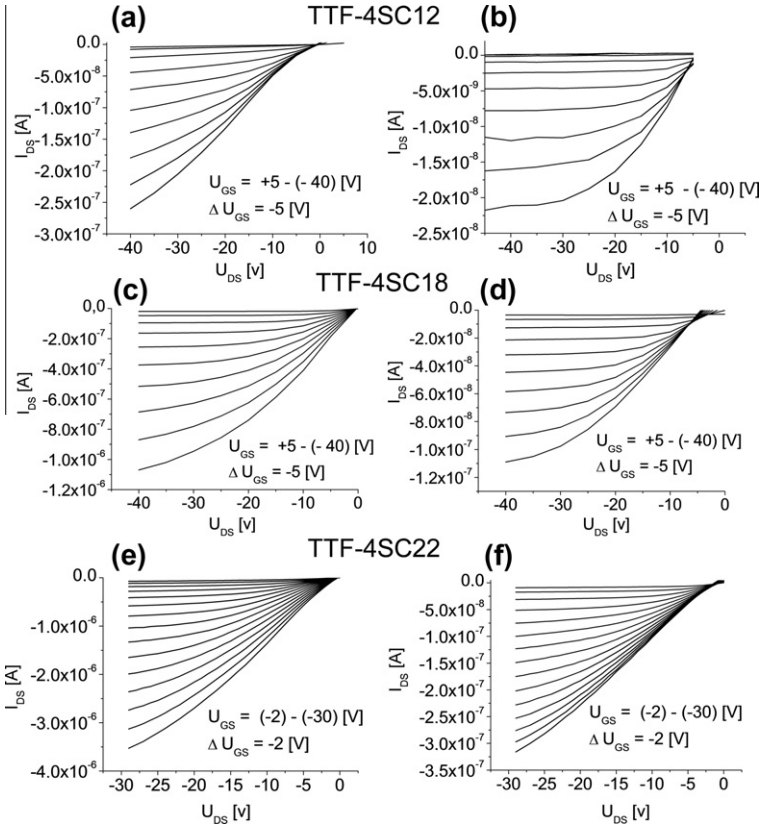

Fig. 9. Output characteristics for FETs made of TTF-4SC$_n$ zone-cast on Parylene C with channel length parallel (left column: a, c, and e) and perpendicular (right column: b, d, and f) to the casting direction.

Table 1
FET charge carrier mobility for TTF derivatives zone-cast on Parylene C dielectric.

	TTF-4SC12	TTF-4SC18	TTF-4SC22
$\mu_{FET\|\|}$ (cm^2/V s)	0.004	0.01	0.1
$\mu_{FET\perp}$ (cm^2/V s)	0.0005	0.001	0.006
ON/OFF	1×10^2	10^2–10^3	1×10^3
SS	1×10^{-5}	2×10^{-5}	6×10^{-5}
V_{TH} (V)	9	10	2

OFET device parameters extracted as prepared: $\mu_{FET||}$, $\mu_{FET\perp}$ – charge carrier mobility parallel and perpendicular to the casting direction respectively; ON/OFF – on/off ratio, SS – subthreshold slope, V_{TH} – threshold voltage.

The anisotropy of electrical properties of the zone-cast TTF layers manifests in very different OFET characteristics with the channel (L = 80 μm and W = 2 mm) oriented parallel and perpendicularly to the casting direction (Fig. 9). The charge carrier mobility calculated on a basis of the transfer characteristics with channel parallel and perpendicular to the casting direction are summarized in Table 1. One can observe an increase of the charge carrier mobility and anisotropy with increasing the alkyl chain length, reaching $\mu_{FET||}$ = 0.10 cm^2/V s for the OFET with TTF-4SC$_{22}$.

The influence of bending on device performance was tested for the OFETs based on TTF-4SC$_{22}$ as active material and Parylene C as dielectric. The flexible OFETs were bent

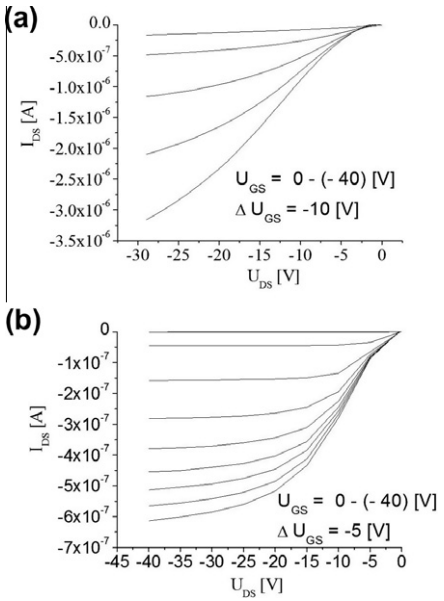

Fig. 10. Output characteristic of FET based on TTF-4SC$_{22}$ on Parylene C during bending test, on roller with curvature radius: (a) r = 25 mm and (b) r = 5 mm.

using rollers with different radius of curvature perpendicular to the channel and casting direction. During the bend-

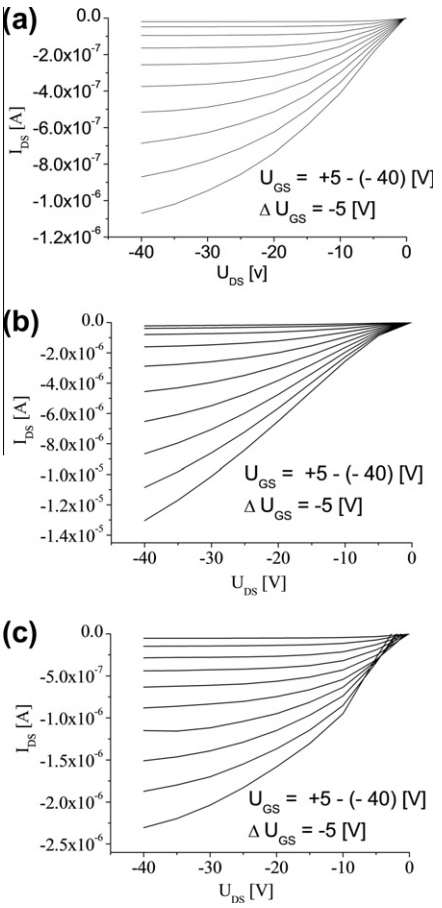

Fig. 11. Effect of atmosphere on performance of OFET based on TTF-4SC$_{18}$ zone-cast on Parylene C with channel length parallel to the casting direction. The output characteristics were obtained for the same device: (a) soon after the fabrication, $\mu = 0.01$ cm^2/V s; (b) after 24 h in ambient conditions (relative humidity: RH ~28–36%) $\mu = 0.17$ cm^2/V s; (c) after annealing at 80 °C in vacuum for 4 h; $\mu = 0.02$ cm^2/V s.

ing the OFET characteristics were measured (Fig. 10). One can see, that after bending the devices are still working, however the calculated mobility is gradually decreasing. The μ_{FET} after bending on a roller with a radius of $r = 25$ mm has decreased from 0.1 cm^2/V s to ca. 0.06 cm^2/V s and it has decreased further to $\mu_{FET} = 0.04$ cm^2/V s for $r = 5$ mm. This effect can be explained by stresses induced in the TTF crystalline films. The drain current is still relatively. Further decreasing of the bending radius ($r < 5$ mm) leads to the drop of charge carrier mobility below 50% of the initially values. Sekitani et al. [18], has reported similar results for the not encapsulated organic transistors based on another small molecular weight semiconductor – pentacene – for which the damage occurs at bending radius ca. 3.5 mm.

A strong increase of the source–drain current was observed when the device was exposed to ambient condition for several hours. It was found that also the off current was increasing. An influence of the ambient atmosphere on the performance of OFETs based on different organic semiconductors was reported already earlier [19–21]. Fig. 11a shows the characteristic measured as prepared for OFET based on zone-cast TTF-4SC$_{18}$ on Parylene C with channel length parallel to the casting direction, and a charge carrier mobility of about 0.01 cm^2/V s was calculated in the saturation regime. Fig. 11b shows the same device after storage under ambient conditions for 24 h. An increase of the source–drain current I_{DS} was observed and also the off current increased (not clearly observable in this scale). The mobility calculated for this device was about 0.17 cm^2/V s in the saturation regime (however this value might be overestimated due to the poor characteristics and lack of clearly seen saturation). Fig. 11c shows the same device after annealing at 80 °C under vacuum for about 4 h. The device characteristics show again lower source-drain currents and also lower off current similar to the first measurements. The mobility for this device in the saturation regime was found to be 0.02 cm^2/V s, it means close to the initial value for fresh device. Thus, we can affirm that although some doping is observed with time, it is possible to reversibly undope it reaching again the initial device performance.

4. Conclusion

It was found, that the zone-cast technique applied for the TTF-4SC$_n$ derivatives yields the best results (continuous and highly oriented layers on large surface) using smooth and homogeneous substrates. Any irregularity (geometrical or chemical) of the substrate surface disturbs the unidirectional growing of the TTF-4SC$_n$ layer.

We have shown, that the Parylene C substrate allows to produce large areas of continuous and well oriented layers of TTF-4SC$_n$. Parylene C appeared to be a promising material for both substrate and gate dielectric in OFET applications. Devices made with such systems are not only flexible but show also superior performance (higher charge carrier mobility) in comparison to the devices based on Si/SiO$_2$ substrates [22].

The performance of OFETs based on TTF-4SC$_n$ and Parylene C is improving with increasing length of alkyl chain in the TTF derivatives. The highest mobility, $\mu_{FET||} = 0.1$ cm^2/V s was found for OFETs with TTF-4SC$_{22}$. This can be explained by the fact, that longer alkyl chain play more effectively role of 'molecular fastener' according to the concept introduced by Inokuchi et al. [23]. Thus, by decreasing the distance between the TTF core in the neighboring molecules this leads to increasing the π–π overlapping as well as close sulfur–sulfur contacts in the quasi 1-dimensional orientation.

Interesting, reversible effect of increasing the source to drain current, and possibly also the field effect mobility, upon exposition to air has to be investigated in more details from the point of view of possible application as oxygen or moisture sensors.

Acknowledgements

The authors thank the EU NoE FlexNet (FP7-ICT 247745), EU Large Project One-P (FP7-NMP-2007-212311), Marie Curie Est FuMaSSEC, the DGI (Spain, CTQ2006-06333/BQU and CTQ2010-19501), the Generalitat de Catalunya (2009SGR00516), Networking Research Center on Bioengi-

neering, Biomaterials and Nanomedicine (CIBER-BBN) and the bilateral project Poland–Spain (MAT2006-28191-E, HISZPANIA/140/2006) and N° N N209 185436 and Nº N507 399939. We also thank Dr. Elba Gomar-Nadal, Dr. Josep Puigmartí and Dr. David Amabilino for their help and advice.

References

[1] S. Seo, B. Park, P.G. Evans, Appl. Phys. Lett. 88 (2006) 232114.
[2] M. Mas-Torrent, C. Rovira, Chem. Soc. Rev. 37 (2008) 827.
[3] M. Leufgen, O. Rost, C. Gould, G. Schmidt, J. Geurts, L.W. Molenkamp, N.S. Oxtoby, M. Mas-Torrent, N. Crivillers, J. Veciana, C. Rovira, Org. Electron. 9 (2008) 1101.
[4] Y. Takahashi, T. Hasegawa, S. Horiuchi, R. Kumai, Y. Tokura, G. Saito, Chem. Mater. 19 (2007) 6382.
[5] H. Jiang, X. Yang, Z. Cui, Y. Liu, H. Li, W. Hu, Y. Liu, D. Zhu, Appl. Phys. Lett. 91 (2007) 123505.
[6] A. Tracz, J. Ulanski, T. Pakula, M. Kryszewski, P-131986 Polish Patent, 1986.
[7] P. Miskiewicz, M. Mas-Torrent, J. Jung, S. Kotarba, J. Glowacki, E. Gomar-Nadal, D.B. Amabilino, J. Veciana, B. Krause, D. Carbone, C. Rovira, J. Ulanski, Chem. Mater. 18 (2006) 4724.
[8] C.M. Duffy, J.W. Andreasen, D.W. Breiby, M.M. Nielsen, M. Ando, T. Minakata, H. Sirringhaus, Chem. Mater. 20 (2008) 7252.
[9] T. Marszalek, E. Dobruchowska, J. Jung, J. Ulanski, M. Melucci, G. Barbarella, Eur. Phys. J. Appl. Phys. 51 (2010) 33208.
[10] A. Tracz, J.K. Jeszka, M.D. Watson, W. Pisula, K. Müllen, T. Pakula, J. Am. Chem. Soc. 125 (7) (2003) 1682–1683.
[11] P. Miskiewicz, A. Rybak, J. Jung, I. Glowacki, W. Maniukiewicz, A. Tracz, J. Pfleger, J. Ulanski, K. Mullen, Nonlinear Opt. Quantum Opt. 37 (2007) 207–218.
[12] K.N. Narayanan Unni, S. Dabos-Seignon, J.M. Nunzi, J. Mater. Sci. 41 (2006) 317–322.
[13] D. Feili, M. Schuettler, T. Doerge, S. Kammer, T. Stieglitz, Sens. Actuators, A 120 (2005) 101–109.
[14] P. Wu, G. Saito, K. Imaeda, Z. Shi, T. Mori, T. Enoki, H. Inokuchi, Chem. Lett. 441 (1986).
[15] A. Tracz, T. Pakula, J. Jeszka, Mater. Sci. (Poland) 22 (2004) 4.
[16] M. Mas-Torrent, S. Masirek, P. Hadley, N. Crivillers, N.S. Oxtoby, P. Reuter, J. Veciana, C. Rovira, A. Tracz, Org. Electron. 9 (2008) 143.
[17] P. Miskiewicz, S. Kotarba, J. Jung, T. Marszalek, M. Mas-Torrent, E. Gomar-Nadal, D.B. Amabilino, C. Rovira, J. Veciana, W. Maniukiewicz, J. Ulański, J. Appl. Phys. 104 (2008) 054509.
[18] T. Sekitani, U. Zschieschang, H. Klauk, T. Sameya, Flexible organic transistors and circuits with extreme Bendig stability, Nat. Mater 9 (2010) 1015–1022.
[19] S. Hoshino, M. Yoshida, S. Uemura, T. Kodzasa, N. Takada, T. Kamata, K. Yase, J. Appl. Phys. 95 (2004) 5088.
[20] M.S.A. Abdou, F.P. Orfino, Y. Son, S. Holdcroft, J. Am. Chem. Soc. 119 (1997) 4518.
[21] M. Mas-Torrent, D. den Boer, M. Durkut, P. Hadley, A.P.H.J. Schenning, Field effect transistors based on poly(3-hexylthiophene) at different length scales, Nanotechnology 15 (2004) S265.
[22] R. Pfattner, M. Mas-Torrent, I. Bilotti, A. Brillante, S. Milita, T. Marszalek, J. Ulanski, A. Nosal, M. Gazicki-Lipman, M. Leufgen, G. Schmidt, V. Laukhin, J. Veciana, C. Rovira, Adv. Mater. 22 (2010) 4198–4203.
[23] H. Inokuchi, G. Saito, P. Wu, K. Seki, T.B. Tang, T. Mori, K. Imaeda, T. Enoki, Y. Higuchi, K. Inaka, N. Yasuoka, Chem. Lett. (1986) 1263.